Journal of Mathematical Chemistry Vol. 30, No. 4, November 2001 (© 2002)

Computation, properties and resonance topology of benzenoid monoradicals and polyradicals and the eigenvectors belonging to their zero eigenvalues

Gordon G. Cash [a] and Jerry Ray Dias [b]

[a] *Risk Assessment Division (7403), Office of Pollution Prevention and Toxics, US Environmental Protection Agency, 1200 Pennsylvania Avenue, N.W. Washington, DC 20460, USA*

[b] *Department of Chemistry, University of Missouri, Kansas City, MO 64110-2499, USA*

Received 26 March 2001

Dedicated to the 80th birthday of Professor Frank Harary

Radical benzenoid structures, i.e., those which cannot have all electrons paired, are known to possess much larger structure counts than closed-shell benzenoids of similar size. Building on our previous work, we report methods for calculating eigenvectors, eigenvalues, and structure counts for benzenoid radicals, diradicals, and radicals of higher multiplicity. When a series of such species is constructed by repeated addition of an aufbau unit, structure counts can usually be expressed as a polynomial in one or two variables. Structure counts for radical series generated by repeated circumscribing, however, cannot.

KEY WORDS: benzenoid radicals, zero eigenvalues, structure count, matching polynomial

AMS subject classification: 92E10

1. Introduction

The classical paper of Gordon and Davison on resonance topology stimulated the research of numerous investigators [1]. Although, in the abstract of this paper, it was stated that “In this first of two papers …”, the sequel which was to deal with non-Kekuléan (radical) benzenoid systems was never published. The study of non-Kekuléan benzenoid systems has become increasingly more important for our understanding of transient reaction intermediates [2], as sources of observed interstellar diffuse spectral bands [3], and as candidates for organic ferromagnets [4].

Hückel molecular orbital (HMO) theory has the following advantages over ab initio quantum mechanical calculations: (1) simple – calculations are not computer-intensive; this permits one to more easily study trends in large sets of molecules; (2) pedagogically favorable – facilitates conceptualization and understanding of chemical phenomena; (3) capable of being quantitative – HMO is tantamount to a quantum-mechanics-based topological index for QSAR studies in molecular modeling; (4) (sometimes) compatible with exact solutions – analytical expression can frequently be formulated for series of related molecular systems. Moreover, the relative signs of the coefficients of the HMO wave functions (eigenvectors) and the order of their size agree with those given by ab initio calculations. Because of these items mentioned above, the discussion sections of ab initio papers are invariably framed in terms of HMO jargon and descriptions.

Eigenvectors (HMO wave functions) of a molecular graph can be partially or fully deduced from the Coulson's pairing theorem [5], Hall subgraphs [6], McClelland subgraphs [7,8], Longuet–Higgens' equation [9], Kassman's path deletion method [10], and Mukherjee and Datta's vertex deletion method [11]. While reviewing some of these methods, new results for obtaining the eigenvectors for the zero eigenvalues of benzenoid monoradicals and polyradicals will be presented.

2. Results and discussion

2.1. Pairing theorem

If the two eigenvalues (X) within a single molecular graph or two related mirror-plane fragment graphs sum to zero ($X_k + X_{N-k+1} = 0$), they are said to be paired. The well-known pairing theorem states that all eigenvalues in a conjugated alternant hydrocarbon (AH) are either zero (nonbonding = NBMO) or paired (bonding = BMO and antibonding = AMO). AHs have no odd-size rings, and every other carbon vertex can be starred so that no two starred and no two unstarred positions are adjacent. If the number of starred and unstarred sites cannot be made equal, then the starred set is selected to be the major set. The eigenvector coefficients for the starred positions of the AH are unchanged in going from one (BMO) eigenvalue (X_k) to its paired (AMO) partner (X_{N-k+1}), and for the unstarred positions the sign (but not magnitude) changes in going from one eigenvalue to its paired partner; if an eigenvalue has no paired partner (i.e., $X = 0$), then the coefficients of the unstarred positions are zero.

Theorem 1. An AH has eigenvalues that are either $X_0(\text{NBMO}) = 0$ or $X_k(\text{BMO}) + X_l(\text{AMO}) = 0$.

Theorem 2. If one of the eigenvectors $\Phi(X_k)$ is given by

$$\Phi(X_k) = \sum_i a_i^* \phi_i^* + \sum_i a_j^\circ \phi_j^\circ$$

where ϕ_i^* is the p AO of a starred atomic vertex and ϕ_j° that of an unstarred atomic vertex, then the eigenvector of its twin $\Phi(X_l)$ is given by

$$\Phi(X_l) = \sum_i a_i^* \phi_i^* - \sum_j a_j^\circ \phi_j^\circ .$$

Theorem 3. The eigenvector for a nondegenerate zero eigenvalue ($X_0 = 0$) is given by

$$\Phi(X_0) = \sum_i a_i^* \phi_i^* .$$

Via the pairing relationship, once all the bonding MOs are known, then the antibonding MOs can be obtained by inspection and vice versa.

2.2. Hall subgraphs

Commonly recurring eigenvalues can be detected by embedding and mirror-plane fragmentation; embedding and right-hand mirror-plane fragments are called Hall and McClelland subgraphs, respectively [6–8]. Hall's descriptive rules for embedding smaller subgraphs onto larger graphs are as follows: (1) all vertices connected to the subgraph fragment must be nodes (zero-eigenvector coefficients); (2) on the other side of each of these nodes must be a repetition of the fragment with the opposite sign; (3) other branches at these nodes will also be nodes. The eigenvectors of the eigenvalues belonging to the embedded subgraphs together are the eigenvectors of the larger molecular graph renormalized by $1/\sqrt{n}$ where n is the number of embedded subgraphs. Embedding occurs most commonly on AHs and in some cases becomes equivalent to mirror-plane fragmentation. A list of common embedding fragments (or MO functional groups) and their corresponding eigenvectors can be found in several sources [11].

2.3. McClelland subgraphs and complementarity

McClelland's rules [7,8] for mirror-plane fragmentation have been reviewed several times. Since we are only concerned with right-hand mirror-plane fragments, one will only need to remember the following: When an internal mirror plane of symmetry divides a molecular graph into two parts, the vertices on the mirror plane remain with the left-hand fragment and vertices in the right-hand fragment originally attached to these vertices have normal weights; vertices in the right-hand fragment originally connected by a bisected edge have weights of -1. Thus, the vertices in the right-hand fragment are either normal or have weights of -1; the latter will be indicated on the fragment graphs by open circles. The McClelland mirror plane defines an antisymmetric relationship for the eigenvectors corresponding to the eigenvalues belonging to the right-hand mirror-plane fragments; in this case, the vertices on the mirror plane have zero eigenvector coefficients. Mirror-plane fragmentation that does not bisect edges is equivalent to embedding with two subgraphs. Most of the right-hand mirror-plane fragments (or MO functional groups) having six or fewer vertices with their eigenvalues and characteristic polynomials have been listed [7,8].

If two eigenvalues in a single molecular graph, a single right-hand mirror-plane fragment, or two related molecular graphs or right-hand mirror-plane fragments sum to minus one ($X_1 + X_2 = -1$), they are said to be *complementary* [7]. Two equal-sized right-hand mirror-plane fragments are complementary if all their eigenvalues are complementary; the normal vertices of one of the complementary right-hand fragments correspond to -1 weighted vertices in the other. Both have the same sets of normalized eigenvector coefficients whose relative sign are fixed for the starred positions but change for the unstarred ones in going from one to the other. Two AH molecular graphs are complementary if their right-hand mirror-plane fragments containing normal and -1

weighted vertices are complementary. If a molecular graph has a right-hand mirror-plane fragment that contains an equal number of normal and -1 weighted vertices which when interchanged gives the same fragment, then both this molecular graph and its right-hand fragment are said to be *self-complementary*. For a given eigenvalue, the McClelland mirror plane of symmetry defines an antisymmetric relationship among the coefficients of the relevant eigenvector.

Let a given right-hand mirror-plane fragment be designated by M and its complement by $\underline{M}$. If k is the index number of a specified starred position of normal weight in M, then k is also the index number for the same starred position of -1 weight in $\underline{M}$; starred normal weighted vertices in M become starred -1 weighted vertices in $\underline{M}$.

Theorem 4. The associated eigenvalues (X) of two complementary right-hand mirror-plane fragments are related by $X(M) + X(\underline{M}) = -1$.

Theorem 5. If the eigenvector $\Phi(M)$ of a right-hand mirror-plane fragment is given by

$$\Phi(M) = \sum_i a_i^* \phi_i^* + \sum_j a_j^\circ \phi_j^\circ \quad \text{for eigenvalue } X(M)$$

where ϕ_i^* is the p AO of a starred atomic vertex and ϕ_j° that of an unstarred atomic vertex, then the eigenvector of its complement is given by

$$\Phi(\underline{M}) = \sum_i a_i^* \phi_i^* - \sum_j a_j^\circ \phi_j^\circ \quad \text{for eigenvalue } X(\underline{M}).$$

Once half the eigenvalues/eigenvectors of an AH molecular graph have been calculated, then the pairing relationship allows one to obtain the remaining values by inspection. Similarly, from the complementary relationship, if the eigenvalues/eigenvectors of one complementary molecular graph are known, then these quantities for the other can be obtained without calculation.

Theorem 6. If $M = \underline{M}$, then M is self-complementary.

Once of the eigenvalues/eigenvectors of an such a AH molecular graph are known, then the complementary and pairing relationships allow one to automatically obtain the remaining quantities.

2.4. Longuet–Higgens equation and the zero sum rule

The basic equation that will be used herein was first given by Longuet–Higgens, but its graph theoretical application has been largely overlooked. The basic algorithm used consists of successive application of the equation $(-X_i C_{iu} + C_{ir} + C_{is} + C_{it} = 0)$ in a systematic fashion to every carbon vertex of a given molecular graph [9]. Each carbon vertex u in a conjugated polyene can be linked either to one (r), two $(r$ and $s)$, or three $(r, s,$ and $t)$ neighboring carbon verices. If carbon vertex u is joined solely to carbon vertex r, then $X_i C_{iu} = C_{ir}$. If u is joined to carbon vertices r and s, $X_i C_{iu} = C_{ir} + C_{is}$. If u is joined to carbon vertices $r, s,$ and t, then $X_i C_{iu} = C_{ir} + C_{is} + C_{it}$. In the application of this algorithm, when available, one should ideally start with a degree -1 vertex and take advantage of molecular symmetry. Since each carbon atom gives rise to one equation, this algorithm generates N_c equations in N_c unkowns that can be solved, if the eigenvalue X_i is specified and the first carbon vertex is arbitrarily assigned $C_{iu} = 1$. Normalization leads to the corresponding wave function coefficients.

There are two special cases for this equation. When $X_i = 0$, this equation reduces to the well-known *zero-sum rule* which can be coupled with the above algorithm to obtain the corresponding eigenvectors (wave function) for the NBMO's. The zero-sum rule states that for the NBMO eigenvector, the coefficients of all the starred positions connected to any given unstarred one must sum to zero. Also, $C_{iu} = 0$ is a condition for embedding. The application of Hall's descriptive rules [6] is an exploitation of the properties of AHs and Longuet–Higgens equation [9].

2.5. Series of monoradicals and their eigenvectors

The benzo[*de*]acene monoradical series (figure 1) were generated by starting with phenalenyl and repetitively attaching the C_4H_2 aufbau unit. The relative eigenvector coefficients for the zero eigenvalue of (odd carbon) AH monoradicals can be obtained by systematic vertex deletion and determination of the number of Kekulé structures (K) of the successor (even carbon) molecular graph. By this method the unnormalized eigenvector for each member of the series in figure 1 was determined. From the eigenvector regularity present for the members shown in figure 1, one can easily determine the successive eigenvectors subsequent members not shown. The sum of the absolute values of these eigenvector coefficients is equal to Herndon's corrected structure count (CSC) [12]. An analytical expression for the CSC of the benzo[*de*]acene series is presented (figure 1).

Figure 2 lists a monoradical series generated starting with phenalenyl by repetitive attachment of the C_6H_2 aufbau unit. The unnormalized eigenvector for the zero eigen-

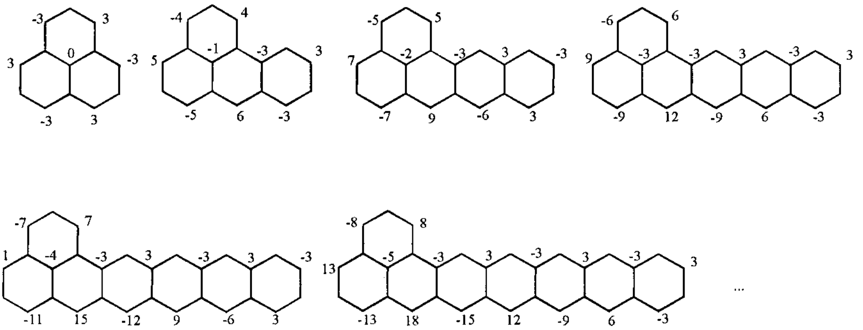

$$\mathrm{CSC} = (1/2)(3n^2 + 23n + 10)$$

Figure 1. Series of benzenoid monoradicals and their eigenvectors for the eigenvalue of zero. The coefficients are the K values of the even carbon successor molecular graph obtained by vertex deletion. The sum of the absolute values of these eigenvector coefficients gives Herndon's corrected structure count (CSC).

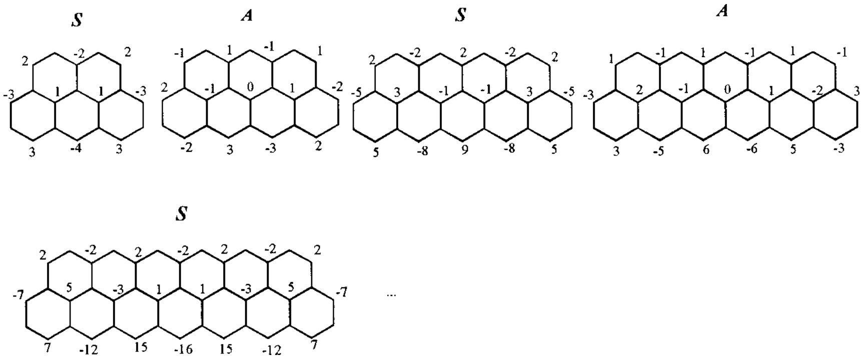

A = antisymmetric case = n = odd; CSC = $(1/2)(n^4 + 11n^3 + 53n^2 + 97n + 54)$; $n = 1$ for phenalenyl
S = symmetric case = n = even; CSC = $(1/2)(n^4 + 11n^3 + 53n^2 + 100n + 60)$

Figure 2. A series of benzeniod monoradicals and their reduced unnormalized eigenvectors for the eigenvalue of $X = 0$.

value is shown for each member. Phenalenyl monoradical, the first generation member ($n = 1$) is not shown, but it has an antisymmetric eigenvector of ones of alternating sign on perimeter degree-2 vertices and a zero at the central degree-3 vertex. The eigenvector pattern in figure 2 alternates between antisymmetric (A) and symmetric (S) where the former has an upper edge of 1's and a central zero and the latter has an upper edge of 2's. The largest coefficients are invariably the lower solo carbon vertices which identify these as the most chemically reactive sites consistent with the known derivatives. After the eigenvectors of the initial members of such a series are generated, it is an easy task to use the pattern to quickly arrive at the eigenvectors of later members. Analytical expressions for the CSC are given in figure 2.

Eigenvectors for zero eigenvalues of AH monoradicals can be determined in a straightforward manner by systematic vertex deletion and determination of the number of Kekulé structures (K) of the successor graph. Consider successive deletion of all the starred vertices in the maximally starred molecular graph of benzo[*cd*]pyrene (figure 3). Deletion of vertices 2 or 10 gives a successor molecular graph having $K = 4$, deletion of vertices 3, 5, 7, or 9 give either the molecular graph of 1- or 4-vinylpyrene having $K = 6$, deletion of vertex 6 gives the molecular graph of benzo[*c*]phenanthrene having $K = 8$, and deletion of vertex 11a gives the molecular graph of 1,8-divinylanthracene having $K = 4$. These K values give the eigenvector coefficients for the respective positions as shown on the tenth structure in figure 3. The values for the remaining internal vertices are obtained by application of the zero sum rule as shown of the eleventh structure in figure 3. Division of these values by two gives the reduced unnormalized eigenvector shown on the twelfth structure. Note that the sum of the absolute values of the unreduced eigenvector (before division by two) gives the CSC = 48.

Using Hall's embedding method, it can be shown that all the molecular graphs in figure 1 can be embedded two distinct ways by ethene and are, therefore, at least doubly degenerate in its eigenvalues of ±1. All the molecular graphs in figure 2 can be embedded once by ethene and have at least one eigenvalue pair of ±1. McClelland's

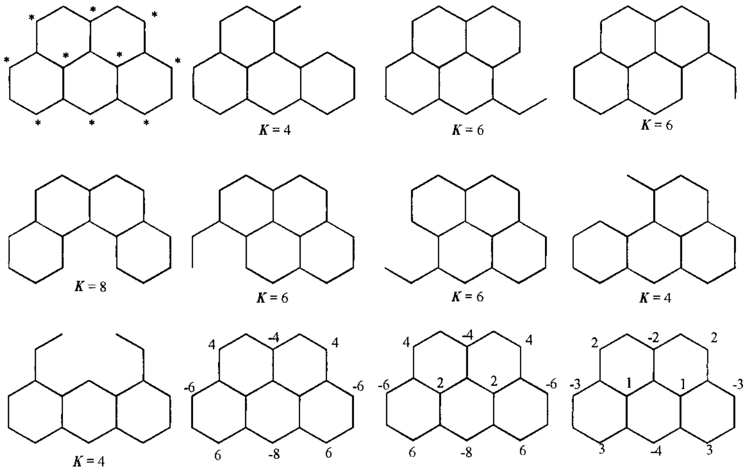

Figure 3. Illustration of the step-by-step procedure for deriving the unnormalized eigenvector for the eigenvalue $X = 0$ of monoradicals. (1) Maximally star the molecular graph. (2) Successively delete each starred perimeter vertex and determine the number of Kekule' structures (K) of the successor graph. (3) Assign the numerical value of K to the deleted vertex. (4) Using the zero-sum rule assign numerical values to the internal third degree vertices. (5) If possible, reduce the numerical values to the smallest integer values, but note that the CSC is given by the sum of the absolute values of the unreduced eigenvector.

mirror-plane fragmentation of the symmetric molecular graphs in figure 2 give right-hand fragments that are nonradical carriers of the ± 1 eigenvalues. Similarly, the right-hand mirror-plane fragments of the antisymmetric molecular graphs are monoradical carriers of the zero and ± 1 eigenvalues; furthermore, the eigenvectors of these fragment monoradicals are obtained directly from the antisymmetric eigenvectors of the precursors.

2.6. *Series of diradicals and their eigenvectors*

Figure 4 lists the diradical series generated from triangulene by repetitive attachment of the C_8H_2 aufbau unit. By ethene embedding, it can be shown that all the molecular graphs in figure 4 have at least eigenvalues of ± 1. It can be seen that mirror-plane fragmentation of the third molecular graph in figure 4 gives a right-hand fragment identical with benzo[*de*]anthracene, the second molecular graph in figure 1 with precisely the same eigenvector.

Benzenoid diradicals have two zero eigenvalues and two unpaired pπ-electrons that are only found on the starred set of carbon vertices. In order for benzenoid diradicals with molecular graphs of two-fold symmetry to have orthogonal eigenvectors for degenerate (zero) eigenvalues, one eigenvector must be symmetrical and the other must be antisymmetrical as shown for the series in figure 4. Mirror-plane fragmentation of a benzenoid diradical gives a right-hand fragment which is a monoradical that identifies the antisymmetric eigenvalues of the diradical precursor. This property can be exploited to easily generate the antisymmetric eigenvector as shown in figure 5 for

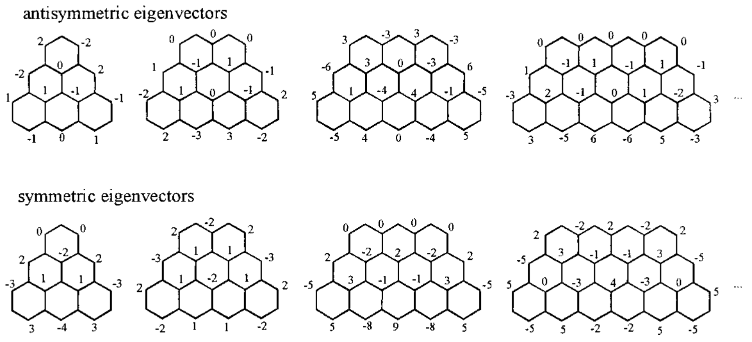

Figure 4. The unnormalized antisymmetric and symmetic eigenvectors of the triangulene diradical benzenoid series for the eigenvalues of X = 0.

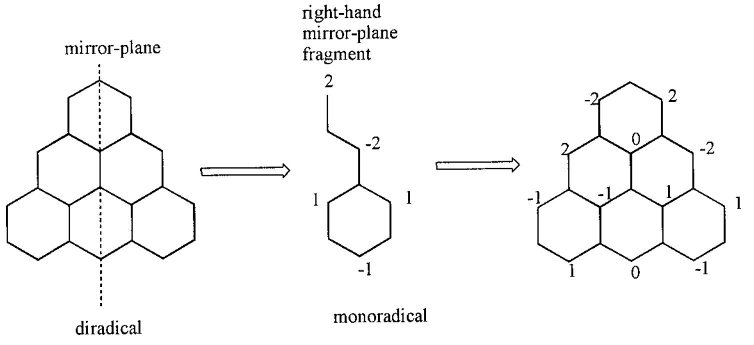

Figure 5. Determination of the antisymmetric eigenvector for the zero eigenvalue of triangulene.

triangulene ($C_{22}H_{12}$). Once the antisymmetric eigenvector is generated, one can easily obtain the corresponding symmetric eigenvector by using a combination of the zero-sum rule, symmetry, and orthogonality.

Compare of the monoradical series in figure 2 with the diradical series in figure 4. Note that, starting with the first member (triangulene) of the symmetric series, the second molecular graph member of the antisymmetric series, the third molecular graph member of the symmetric series, the fourth member of the antisymmetric series, and so forth, all the diradicals in figure 4 with zero coefficients at the top of every other molecular graph alternate between the symmetric and antisymmetric series. If one disregards the zero coefficients of triangulene in figure 4, it is seen that the remaining coefficients exactly match those in benzo[*cd*]pyrene (first molecular graph) in figure 2. A similar matching between the molecular graphs in figure 4 topped with zero coefficients and the remaining molecular graphs in figure 2 should be evident.

The pattern established between the eigenvectors of the benzenoid monoradical series in figure 2 and the diradical series in figure 4 arises from the antisymmetric/symmetric and zero-sum properties of peaks belonging to two-fold symmetrical benzenoid diradicals. In general, two-fold symmetrical benzenoid diradicals having a triangular or trapezoidal shape with an odd number of continuously connected peaks will

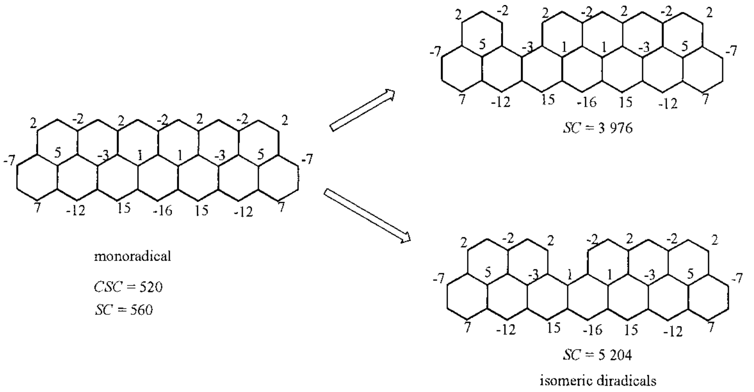

Figure 6. Unstarred peak deletion converts a monoradical into a diradical in which one of the zero eigenvalues has the original (unnormalized) eigenvector.

have a cap of zero coefficients for their symmetrical eigenvectors or with an even number of continuously connected peaks will have a cap of zero coefficients for their antisymmetrical eigenvectors corresponding to one of two of the zero eigenvalues. One of the eigenvectors to some molecular graphs of benzenoid diradicals related to the structures in figure 2 can be obtained directly from them by judicious deletion of unstarred peaks as illustrated in figure 6. Such deleted of unstarred peaks are models for point defects in quasi-graphite strips [4]; figure 6 suggests that these point defects should both increase the number of charge carriers (radical multiplicity) and the width of the conduction band which *SC* is a measure.

2.7. Corrected structure count (CSC)

Resonance predictions of the relative stability of isomeric species are invariably based on the number of valence-bond structures can be drawn for them. Structure count (SC) is the total number of valence-bond structures that can be written for any given conjugated pπ-system whether it is an ionic, radical, or molecular species. Kekulé structure count (in mathematical jargon, number of unique 1-factor subgraphs) is the term used for alternant hydrocarbons. Corrected structure count (CSC) was defined by Herndon as the structure count exclusive of (anti-aromatic) structures which do not contribute to stabilizing resonance interactions [12]. The determination of SC and CSC can be illustrated by the biphenylene and phenalenyl examples in figure 7. The square-root of the tail coefficient of the characteristic polynomial of even-carbon alternant hydrocarbons (EAH) gives the CSC which equals the SC if the alternant hydrocarbon contains no anti-aromatic $4n$ rings. The square-root of the tail coefficient to the characteristic polynomial of biphenylene gives CSC $= 3$; of course, the square-root of the sum of the squares of all the eigenvalues (roots) of this characteristic polynomial also gives CSC $= 3$. Using Herndon's vertex deletion method [12] on biphenylene gives an odd alternant hydrocarbon (OAH) on which the application of the zero-sum rule, one obtains the unnormalized eigenvector coefficients for the NBMO of the OAH as shown in

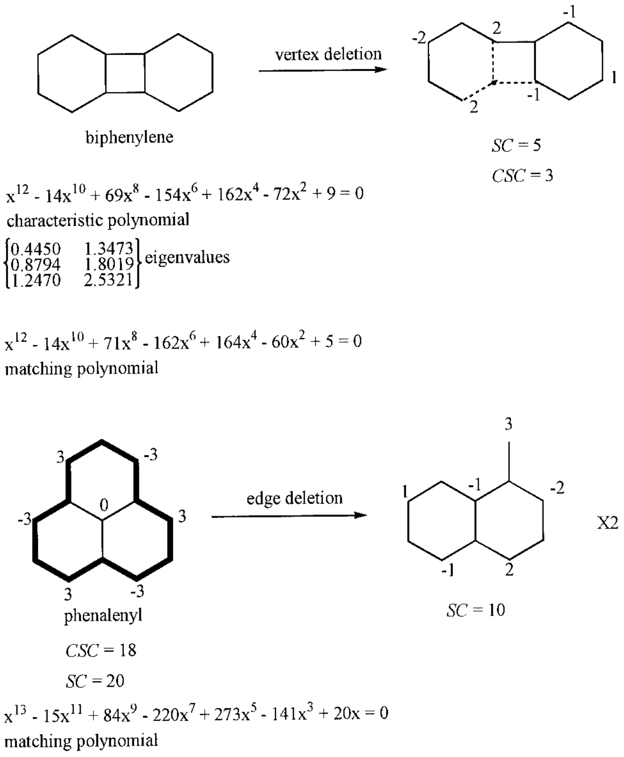

$SC = 5$

$CSC = 3$

$x^{12} - 14x^{10} + 69x^8 - 154x^6 + 162x^4 - 72x^2 + 9 = 0$
characteristic polynomial

$\begin{Bmatrix} 0.4450 & 1.3473 \\ 0.8794 & 1.8019 \\ 1.2470 & 2.5321 \end{Bmatrix}$ eigenvalues

$x^{12} - 14x^{10} + 71x^8 - 162x^6 + 164x^4 - 60x^2 + 5 = 0$
matching polynomial

$SC = 10$

$CSC = 18$

$SC = 20$

$x^{13} - 15x^{11} + 84x^9 - 220x^7 + 273x^5 - 141x^3 + 20x = 0$
matching polynomial

Figure 7. SC for any molecular graph is determined from the value of the tail coefficient to its matching polynomial. CSC is obtained by excluding the antiaromatic contributions to SC.

figure 7. The sum of the absolute values of the coefficients to the vertices which were attached to the deleted vertex gives the SC of the biphenylene precursor and the algebraic sum gives the CSC.

The tail coefficient of the matching polynomial of any molecular graph always gives the SC directly. The CSC of monoradical OAHs with antiaromatic rings requires a different approach from Herndon's method [12] as illustrated with phenalenyl in figure 7. The tail coefficient to the characteristic polynomial of phenalenyl monoradical gives no information on CSC. Using the vertex deletion/zero-sum procedure outlined in figure 3, the unreduced eigenvector coefficients shown in figure 7 were obtained. The sum of the absolute values of these coefficients gives CSC $= 18$ for phenalenyl. In the set of all phenalenyl resonance structures, a double bond must be either at edge *a* or edge *b*. Deletion of either edge along with the pendent vertices gives the α-methylenylnaphthalene structure with a SC $= 10$ as shown. Thus, the phenalenyl predecessor has a SC $= 2 \cdot 10 = 20$ in agreement with the tail coefficient of the matching polynomial. The reduction of SC by two to give CSC arises in phenalenyl because the former counts the anti-aromatic perimeter where the unpaired electron is localized on the central internal vertex, whereas the eigenvector coefficient of zero at this point tells us that the unpaired electron is never localized at the position.

There are two methods to obtain the CSC for monoradicals. The first method is illustrated in figure 3 uses a vertex deletion/zero-sum rule procedure to compute the unnormalized eigenvector for the corresponding zero eigenvalue. The second method uses the tail coefficient of the matching polynomial amended by antiaromatic contributions determined by select Sachs' graphs as we now discuss. Let the tail coefficient to the characteristic polynomial of an odd carbon ($N = N_c$) monoradical be a_{N-1}, then

$$a_{N-1} = a_{N-1}(\text{acyclic}) + a_{N-1}(\text{cyclic})$$

where $|a_{N-1}(\text{acyclic})| = \text{SC}$ is the tail coefficient of the matching polynomial. It follows that

$$a_{N-1}(\text{cyclic}) = a_{N-1}(\text{aromatic}) + a_{N-1}(\text{antiaromatic})$$

and

$$a_{N-1}(\text{antiaromatic}) = a_{N-1}(\boldsymbol{C}_{4n},\ n = 3) + a_{N-1}(\boldsymbol{C}_{4n},\ n > 3)$$

where $a_{N-1}(\boldsymbol{C}_{4n},\ n = 3)$ includes $\boldsymbol{C}_{12}$ circuit components; note that a_{N-1} [and a_{N-1}(acyclic)] and a_{N-1}(antiaromatic) will always have opposite signs and that $\boldsymbol{C}_{12}$ is the smallest antiaromatic circuit that can be found in a benzenoid radical system. Thus

$$\text{CSC} = \left|a_{N-1}(\text{acyclic}) + a_{N-1}(\boldsymbol{C}_{4n},\ n = 3)\right|.$$

Overall, Herndon's CSC only subtracts out destabilizing resonance contributions due to the smallest, more important antiaromatic circuit components.

2.8. *Higher radicals*

While the SC of low symmetry diradicals and higher multiplicity radicals can be determined from the tail coefficients of their corresponding matching polynomials or by decomposition methods, general methods for determining their CSC and eigenvectors remain unresolved. Even the meaning of CSC in regard to benzenoid polyradicals remains, at best, vague. Table 1 lists SC values for a number of benzenoid polyradicals. These results were obtained using Mathematica® to find the matching polynomial. The program was adapted from one published by Salvador et al. [13]. Because of the large size of some of the structures in table 1, it was necessary to break the structure into two fragments of approximately equal size and calculate the matching polynomial for the whole according to the equation of Babić et al. [14].

2.9. *Constant-isomer radical series*

The row series in table 1 are all one-isomer series. The first row is the $\boldsymbol{D}_{6h}$ polycircum series generated by repetitive circumscribing starting with benzene. The second row is the $\boldsymbol{D}_{3h}$ polycircumphenalenyl monoradical series, and the third row is the polycircumtriangulene diradical series. Circumscribing methyl radical (CH_3) with a perimeter of $2N_H + 6$ carbons ($N_H = 3$ for methyl) and 6 more hydrogens gives

Table 1

Rows are labeled with multiplicity of the radical, columns with number of times the basic triangular polyradical is circumscribed. Entries consist of the chemical formula for each structure (above) and SC (below). SCs for formulas with no corresponding value could not be determined with available equipment.

	0	1	2	3	4
0	C_6H_6 2	$C_{24}H_{12}$ 20	$C_{54}H_{18}$ 980	$C_{96}H_{24}$ 232 848	$C_{150}H_{30}$ 267 227 532
1	$C_{13}H_9$ 20	$C_{37}H_{15}$ 999	$C_{73}H_{21}$ 189 792	$C_{121}H_{27}$ 153 915 460	
2	$C_{22}H_{12}$ 306	$C_{52}H_{18}$ 59 886	$C_{94}H_{24}$ 39 045 432	$C_{148}H_{30}$ 100 645 429 215	
3	$C_{33}H_{15}$ 7 376	$C_{69}H_{21}$ 5 013 752	$C_{117}H_{27}$ 10 457 948 644	$C_{177}H_{33}$	
4	$C_{46}H_{18}$ 273 956	$C_{88}H_{24}$ 604 073 400	$C_{142}H_{30}$ 3 859 415 491 248	$C_{208}H_{36}$	
5	$C_{61}H_{21}$ 15 345 156	$C_{109}H_{27}$ 105 179 890 458	$C_{169}H_{33}$ 2 000 179 735 422 600		
6	$C_{78}H_{24}$ 1 274 990 124	$C_{132}H_{30}$ 26 398 415 877 712	$C_{198}H_{36}$		
7	$C_{97}H_{27}$ 155 024 945 978	$C_{157}H_{33}$ 9 510 671 755 316 374			
8	$C_{118}H_{30}$ 27 422 185 371 264				
9	$C_{141}H_{33}$ 6 981 850 496 603 886				
10	$C_{166}H_{36}$ 2 547 185 424 690 611 836				

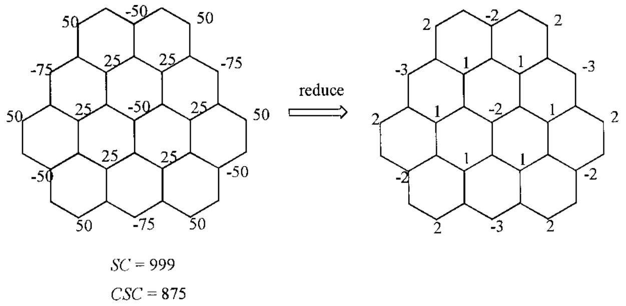

Figure 8. Eigenvector for the zero eigenvalue of circumphenalenyl monoradical.

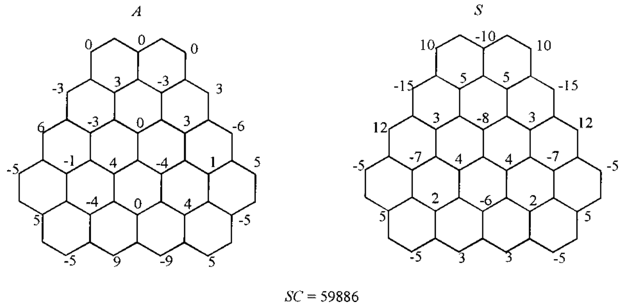

Figure 9. Antisymmetric and symmetric eigenvectors for the zero eigenvalues of circumtriangulene.

phenalenyl monoradical ($C_{13}H_9$); methyl radical is the excised internal structure of phenylenyl. Repetitive circumscribing starting with phenalenyl (first generation member) gives successive members of the $\boldsymbol{D}_{3h}$ one-isomer monoradical series with NBMO eigenvectors that alternate between anti-symmetric and symmetric (confer with figure 8 for the second generation member). While there are three $C_{22}H_{12}$ benzenoid isomers, triangulene (figure 5) is the only diradical isomer. Circumscribing triangulene diradical with $2N_H + 6 = 2 \cdot 12 + 6 = 30$ carbons and 6 more hydrogens gives circumtriangulene ($C_{52}H_{18}$, figure 9), the second generation member of the $\boldsymbol{D}_{3h}$ one-isomer diradical series; the SC values given in this row of table 1 are only for these diradicals. In the fourth row, $C_{33}H_{15}$ is the formula of 17 monoradicals and one triradical, where the latter is the excised internal of the first generation member ($C_{69}H_{21}$) to the $\boldsymbol{D}_{3h}$ triradical series. The SC values given in the fourth row of table 1 are only for the single triradical of each formula. In the fifth row, $C_{46}H_{18}$ is the formula for 187 benzenoid isomers, 22 which are diradicals and one which is a tetraradical; the SC values given in this row are only for the sole tetraradical and the first generation member of the $\boldsymbol{D}_{3h}$ one-isomer tetraradical series has the formula of $C_{142}H_{30}$. All the formulas in the first column correspond to the triangular benzenoid hydrocarbons (figure 10).

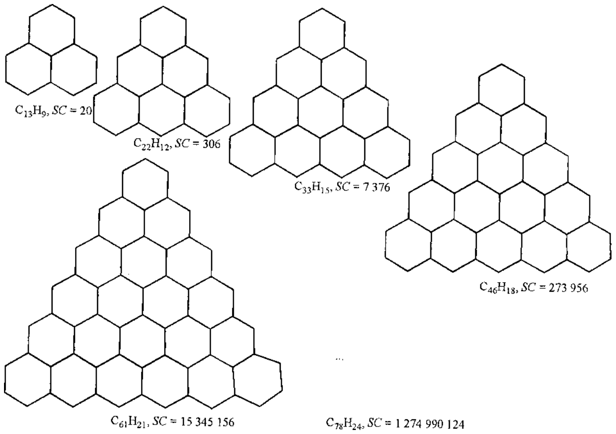

Figure 10. Smallest most condensed benzenoid polyradical series.

2.10. Analytical expressions

It has been demonstrated that whenever a series is generated by repetitive attachment of a given aufbau unit as in figures 1 and 3, then their SC analytical expressions will have a polynomial form as shown [15,16]. Since the $\boldsymbol{D}_{6h}$ one-isomer circumbenzene series (the first row in table 1) has a factorial form for its $K = \mathrm{SC}$, we conjectured that other (radical) series generated by successive attachment of units that are being progressively incremented (growing) or by successive circumscribing as in the construction of constant-isomer series might also have a similar factorial form for their SC analytical expressions. The second type of analytical expression was published by Gordon and Davison [1] with permission by the originator, M. Woodger, who was supposed to subsequently publish his derivation but never did. Gordon and Davidson expressed this value as

$$K = \prod_{i=n}^{2n-1} \binom{n+i}{n} \div \prod_{i=1}^{n-1} \binom{n+i}{n},$$

where the products are over the appropriate binomial coefficients. The on-line encyclopedia of integer sequences [17] identified the sequence as the number of ways to tile a hexagon of edge n with diamonds of edge 1, and also the number of plane partitions whose Young diagrams fit inside an $n \times n \times n$ box. This source expressed the formula as

$$K = \prod_{i=1}^{n}\prod_{j=1}^{n}\prod_{k=1}^{n} \frac{i+j+k-1}{i+j+k-2} = \prod_{i=1}^{n} \frac{\Gamma(i)\Gamma(2n+i)}{[\Gamma(n+i)]^2} = \prod_{i=0}^{n-1} \frac{i!(2n+i)!}{(n+i)!^2}.$$

Our efforts to find similar factorial SC analytical expressions failed. Superseeker [18], which performs many mathematical searches, as well as searching the on-line encyclopedia of integer sequences, found no analytical formula for any row or column from table 1. The fact that the circumbenzene series have SC values with reasonably small

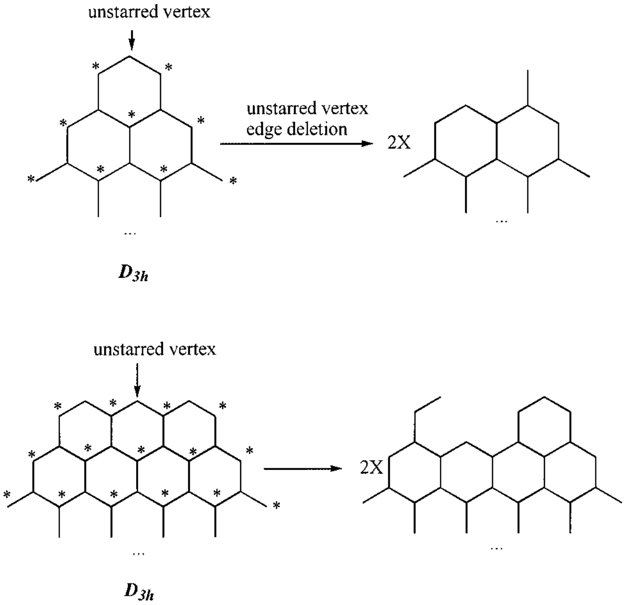

Figure 11. Decomposition of a D3h triangular- or trapezoidal-shaped benzenoid molecular graph by operating on a central unstarred peak per $\mathrm{SC}(G) = \sum \mathrm{SC}(G\text{–}(e))$ proves that all such graphs with an odd number of peaks must have an even SC value.

prime factors (e.g., $267\,227\,532 = 2^2 \times 3^3 \times 11^3 \times 13^2$) whereas the row and column radical series exhibit very large prime factors (e.g., $273\,956 = 2^2 \times 68\,489$ and $189\,792 = 2^5 \times 3^2 \times 659$) suggests that if SC analytical expressions for these series do exist that they will have a very different form from the polynomial and factorial types.

Even though no SC analytical expressions have been found for the mono- and polyradical benzenoid $\boldsymbol{D}_{3h}$ one-isomer series having formulas given in table 1, some general observations can be summarized. Comparing SC values for similar carbon numbers (e.g., the $C_{97}H_{27}$ heptaradical versus $C_{94}H_{24}$ diradical or the $C_{141}H_{33}$ nonaradical versus the $C_{142}H_{30}$ tetraradical) show that the number of resonance structures rapidly increases as the radical multiplicity increases. By way of symmetry, if one decomposes any benzenoid molecular graph having a formula in the first, third, fifth, etc. columns of table 1 by the method illustrated in figure 11, it is proved that their SC values must be even numbered. By Hall's embedding method, it can be shown that all the $\boldsymbol{D}_{3h}$ benzenoid radicals in table 1 are at least triply degenerate in the eigenvalues of ±1.

3. Conclusions

While reviewing descriptive HMO techniques for studying structural properties of radical systems, new eigenvector patterns and SC data for benzenoid series generated by repetitive attachment of a given aufbau unit and by successive circumscribing have been determined. The smallest most condensed benzenoid polyradicals (figure 10) have considerable theoretical importance and their number of resonance structures have been determined and summarized in the first column of table 1. Herndon's CSC has been further analyzed. Since the unpaired electrons in alternant radicals are only found on the starred carbon sites, the starred vertex deletion procedure for obtaining unnormalized eigenvectors for the purpose of determining the CSC of the zero eigenvalue of monoradicals (confer with figure 3) represents a slight improvement over Herndon's original procedure [12].

4. Disclaimer

This document has been reviewed by the Office of Pollution Prevention and Toxics, USEPA, and approved for publication. Approval does not signify that the contents necessarily reflect the views and policies of the Agency, nor does the mention of trade names or commercial products constitute endorsement or recommendation for use.

References

[1] M. Gordon and W.H.T. Davison, J. Chem. Phys. 20 (1952) 428.
[2] A. Keller, R. Kovacs and K.-H. Homann, Phys. Chem. Chem. Phys. 2 (2000) 1667.
[3] S. Leach, Z. Phys. Chem. 195 (1996) 15.
[4] A. Rajca, Chem. Rev. 94 (1994) 871; F. Dietz and N. Tyutyulkov, Chem. Phys. 246 (1999) 255.
[5] J.R. Dias, *Molecular Orbital Calculations Using Chemical Graph Theory* (Springer, Berlin, 1993).
[6] J.R. Dias, Internat. J. Quantum Chem. 74 (1999) 721; G.G. Hall, Inst. Math. Appl. 17 (1981) 70; G.G. Hall, Trans. Faraday Soc. 53 (1957) 573.
[7] J.R. Dias, Molec. Phys. 88 (1996) 407.
[8] B.J. McClelland, J.C.S. Faraday Soc. Trans. II 70 (1974) 1453; B.J. McClelland, J. Chem. Soc. Faraday Trans. 2 78 (1982) 911; B.J. McClelland, Molec. Phys. 45 (1982) 189.
[9] J.R. Dias, Molec. Phys. 85 (1995) 1043.
[10] A.J. Kassman, Theor. Chim. Acta 67 (1985) 2555.
[11] A.K. Mukherjee and K.K. Datta, Proc. Indian Acad. Sci. 101 (1989) 499.
[12] W.C. Herndon, Tetrahedron 29 (1973) 3; W.C. Herndon, J. Chem. Educ. 51 (1974) 10; W.C. Herndon, J. Org. Chem. 46 (1981) 2119.
[13] J.M. Salvador, A. Hernandez, A. Beltran, R. Duran and A. Mactutis, J. Chem. Inf. Comput. Sci. 38 (1998) 1105.
[14] D. Babić, G. Brinkmann and A. Dress, J. Chem. Inf. Comput. Sci. 37 (1997) 920.
[15] J.R. Dias, J. Chem. Inf. Comput. Sci. 40 (2000) 810.
[16] J.R. Dias and G.G. Cash, J. Chem. Inf. Comput. Sci. 41 (2001) 129.
[17] http://www.research.att.com/∼njas/sequences
[18] http://www.research.att.com/∼njas/sequences/ol.html